



Article

Development, Validation, and Evaluation of Partial PST Tractor Simulation Model for Different Engine Modes during Field Operations

Md. Abu Ayub Siddique ¹, Seung-Min Baek ², Seung-Yun Baek ², Yong-Joo Kim ^{1,2,*} and Ryu-Gap Lim ^{3,*}

¹ Department of Agricultural Machinery Engineering, Chungnam National University, Daejeon 34134, Republic of Korea

² Department of Smart Agriculture Systems, Chungnam National University, Daejeon 34134, Republic of Korea

³ Innovalley Substantiation Team, Korea Agriculture Technology Promotion Agency, Sangju 37127, Republic of Korea

* Correspondence: babina@cnu.ac.kr (Y.-J.K.); limso@koat.or.kr (R.-G.L.); Tel.: +82-42-821-6716 (Y.-J.K.)

Abstract: The objectives of this study are the development and verification of a simulation model of the partial PST (power-shift transmission) tractor based on actual field operations. The PST simulation model was verified for the asphalt driving condition, and performance was evaluated for asphalt driving, plow, and rotary tillage. In this study, the traditional, APS (Auto Power Shift) ECO, and APS power engine modes were used to analyze fuel consumption. The statistical analysis proved that the experimental and simulation results were in a linear relationship, with an accuracy of over 98%. Finally, the results suggested that users could utilize the 95-kW partial PST tractor in the APS ECO engine mode with higher fuel economy compared to the traditional and APS power modes.

Keywords: tractor; powershift transmission; tillage; simulation model; fuel consumption



Citation: Siddique, M.A.A.; Baek, S.-M.; Baek, S.-Y.; Kim, Y.-J.; Lim, R.-G. Development, Validation, and Evaluation of Partial PST Tractor Simulation Model for Different Engine Modes during Field Operations. *Agriculture* **2023**, *13*, 44. <https://doi.org/10.3390/agriculture13010044>

Academic Editors: Eugenio Cavallo, Carlo Bisaglia and Francesco Marinello

Received: 24 November 2022

Revised: 17 December 2022

Accepted: 21 December 2022

Published: 23 December 2022



Copyright: © 2022 by the authors. Licensee MDPI, Basel, Switzerland. This article is an open access article distributed under the terms and conditions of the Creative Commons Attribution (CC BY) license (<https://creativecommons.org/licenses/by/4.0/>).

1. Introduction

The agricultural tractor has to perform in various working environments and provide large amounts of traction force at low driving speed. Several new technologies in agricultural machinery, such as unmanned or autonomous vehicles and artificial intelligence, are implemented bearing in mind comfort for the driver, efficiency, and precision [1]. To ensure drivers' flexibility, precise farm operation, and maximized power delivery in each working condition during field operations, academic researchers and manufacturers are continuously developing numerous powertrains for off-road vehicles. Among them, manual transmission (MT), automatic transmission (AT), dual-clutch transmission (DCT), continuously variable transmission (CVT), as well as power shift transmission (PST) are developed for the tractors [2–4].

PST is a precision technology that makes it easy and convenient for users to regulate and maintain the tractor during on-field operations. It can change the gear stages precisely during operation under the load conditions of the tractor [5]. The partial PST tractors deal with the two or more gear stages without using a clutch, although it must have clutched to shift gears. However, the users can shift all gears without using the clutch in the full PST tractors [6]. Neto et al. [7] conducted research on CVT with full powershift (FPS) to improve the efficiency of the agricultural tractor and reported that the FPS was more energy efficient. Therefore, a PST model was proposed considering its high efficiency, smoothness, and wide range of applications (small, medium, and large tractors). In PST, the hydraulic proportional valve is used to regulate and precisely control the hydraulic pressure. The proportional valve also utilizes an electric control signal to engage for delivering power, comfort during driving, and economic efficiency [8]. PST technology is configured with a varied range of speed without loss of power when it delivers from the engine to the driving

axles [1,6,9]. Hence, PST technology can be applied in low- to high-power vehicles and is gaining popularity for being a precise technology.

PST technologies have been designed with at least two or more wet clutches, which are regulated by the pressure supplied from the hydraulic proportional valve through a hydraulic circuit [10–12]. For decades, researchers have mainly been focused on reducing energy losses during engagement or disengagement of the clutches and on smooth and fast clutch engagement for user comfort [13]. Research has been conducted to implement proportional control valves in the agricultural machinery field to enhance performance [14,15]. Raikwar [16] developed the power shuttle system for tractors to regulate the pressure using the proportional control valve to actuate the clutch. He stated that the proportional control valve can engage and disengage the clutch precisely. As there are various factors relevant to the design of the model of the PST, the scholars attempt to identify the factors that influence precise clutch engagement considering fast engagement, smooth shifting, friction, reasonable operating load, and flexible operations.

Li et al. [17] designed a novel power shift transmission to improve performance and minimize manufacturing cost. In this study, coordinated control strategies for the upshift and downshift processes of the multiple clutches during tractor field operation were developed. However, the control strategy was not verified by the field experiment. Yiwei et al. [18] also developed an architecture modeling and high-level architecture (HLA) of the PST. In this study, the dynamic principles of the PST mechanical, hydraulic, and control subsystems were established, where the maximum error between simulation and test was found to be approximately 7.89%. Yang et al. [19] proposed the full power shift method of the HMT, which is divided into five stages (current range, prior stable stage, power transition stage, post stable stage, and target range). Another investigation was conducted on the working principle of the hydraulic valve for PST and evaluated with a bench test [20,21]. Also, the shifting quality improvement of the PST tractor was conducted with a simulation and a control algorithm [22,23]. The wear failure of the gear for PST was also studied [24]. However, there was a lack of field experiments during major agricultural operations.

In addition, Siddique et al. [25] reported that the important factors for hydraulic clutches are, first: sliding velocity [26], second: inertia [27], and finally: heat generation [28]. They developed a simulation model of the hydraulic clutch pack and designed the critical factors for the PST tractor. Also, they evaluated these factors using the hydraulic test bench based on various hydraulic oils of VG 32, 46, and 68 at different temperature levels such as 25, 40, 60, 80, and 100 °C. Siddique et al. [29] studied the fuel efficiency of the PST tractor according to engine load conditions using the indoor test. PTO (power-take-off) dynamometer was used to measure the engine loads and the tractor's fuel consumption was measured by REO-CFMT. However, real agricultural operations were not conducted to validate the tractor simulation model.

In our study, a partial PST tractor simulation model was developed and verified for actual field operations using a real agricultural tractor. In addition, this study was focused on verifying the PST simulation model of the tractor considering major agricultural operations and engine mode. Therefore, the specific goals of our study were as follows: (i) to develop a PST simulation model for a tractor; (ii) to analyze the experimental data for different engine modes; (iii) to validate the simulation model during asphalt driving operation; and (iv) to make a correlation between the simulation and experimental results for major agricultural operations.

2. Materials and Methods

2.1. Partial PST Tractor Specifications

A 95-kW partial PST tractor (T130, TYM Co., Ltd., Gongju, Korea) was the target tractor to evaluate the developed simulation model. The tractor's dimension was 4490 (L) × 2360 (W) × 2940 (H) mm. The rated torque of engine is 415 Nm at 2200 rpm of rated speed. The PST for forward and reverse is combined of 18 × 18 gear stages. The tractor's

gross weight is 44,587 N with distribution ratios for front and rear axles of 40.3 and 59.7%, respectively. The tractor specifications were listed in Table 1.

Table 1. The specifications of the partial power-shift transmission (PST) tractor used in this study.

Parameters	Specifications	
Model	T130, TYM, Korea	
Weight (N)	Gross weight (N)	44,587
	Weight distribution (%)	40.3 and 59.7
Engine	Type	Tier 4
	Rated power (kW)	95
	Rated torque (Nm)	415
	Rated speed (rpm)	2200
	Shifting method	Power-shift
Transmission	Main clutch	3
	Sub-shifting stages	3 (L, M, H)
	Combinations (forward × reverse)	18 × 18
Tire	Model (front and rear)	380/85R24 and 460/85R38
	Diameter (front and rear) (mm)	1256 and 1770

The tractor powertrain is composed of 2 high and low (power shifts), 3 power-shift type main clutches, and 3 mechanical type range shifts. Engine power is generally transmitted to the main clutch which deals with the forward-reverse and high-low shifts. Sequentially, the driving shaft drives the rear PTO connecting with the driving shift gear, range shaft gear, and PTO shift gear. Since the tractor sub-shift is performed with a mechanical gear, it is called the partial PST. The block diagram of the tractor powertrain is shown in Figure 1.

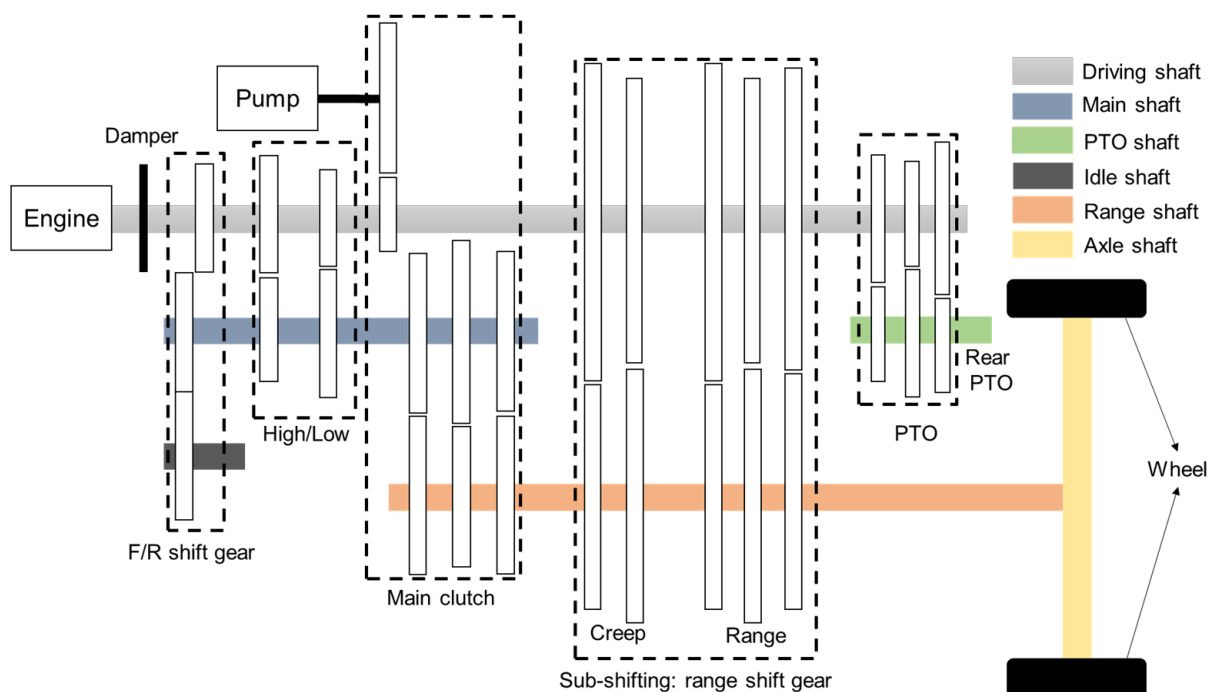


Figure 1. The block diagram of a 95-kW partial PST tractor transmission.

2.2. Partial PST Tractor Simulation Model

The simulation model was developed using the commercial simulation software LMS AMESim (version 16, SIEMENS AG, Munich, Germany) based on the powertrain of the PST tractor. The entire PST tractor simulation model is shown in Figure 2. The simulation

model consists of forward/reverse, Hi/Low, and 3 main clutch packs that are the same structure including several mechanical components. Each clutch pack has a proportional control valve to engage or disengage the clutch. All hydraulic clutch packs are operated by hydraulic pressure supplied from a proportional control valve. The sub-shifting including creep was constructed with mechanical gears. The PTO gear stages were divided in three (P1, P2, and P3).

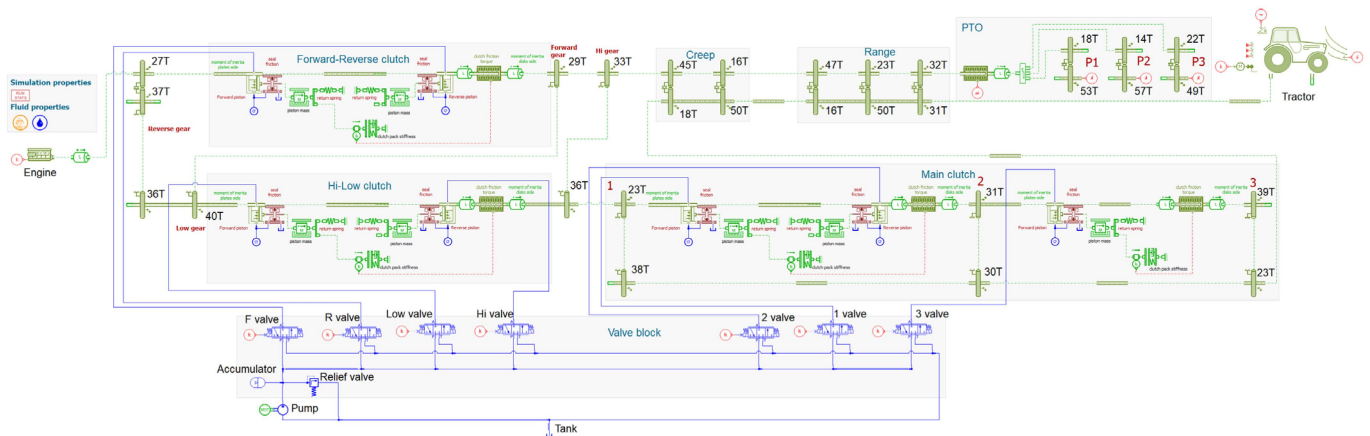


Figure 2. The simulation model of a 95-kW partial PST tractor.

In this model, the hydraulic clutch pack was specified by a previous study [25]. The target tractor is operated by a 95-kW engine. The total engine power is delivered to the main transmission and rear PTO. The main transmission power is delivered to the driving axle dealing with the high-low clutch, main hydraulic clutch pack, and mechanical sub-shifting including creep and range. The tractor model was designed using the tractor's gross weight and tire specifications. In this study, the measured data and engine characteristics map were applied to conduct and verify the simulation model. The axle load, which was measured from real field experiments was also used as an input parameter to characterize field operations such as asphalt driving, plow tillage, and rotary tillage. The specifications of the hydraulic component of the simulation model are listed in Table 2.

Table 2. The hydraulic component specifications of the simulation model.

Parameters	Specifications	
Gear pump	Gear ratio	0.83
	Displacement (cc/rev)	14
	Rotational speed (rpm)	1826
Relief valve	Cracking pressure (bar)	200
Accumulator	Type	Membrane type
	Precharge gas	Nitrogen (N ₂)
	Volume (cc)	320
	Precharge pressure (bar)	15
Proportional valve	Max. current (mA)	1200
	Current signal	User command

2.3. Simulation Conditions

2.3.1. Component Design of the Model

The hydraulic pump was specified with a gear ratio of 0.83, where the displacement volume and rotational speed were 14 cc/rev and 2200 rpm, respectively. The cracking pressure of the relief valve was 200 bar. The gas pre-charge pressure and the accumulator volume were 15 bar and 0.32 L, respectively.

Figure 3a shows the tuning of the relief valve. It can be observed that the relief valve started to open at the cracking pressure and it fully opened when the system pressure was 212.85 bar. The pre-charge pressure of the internal gas and the hydraulic fluid pressure of the accumulator were the same due to the system pressure of the hydraulic system, accounting for almost 212.85 bar, shown in Figure 3b.

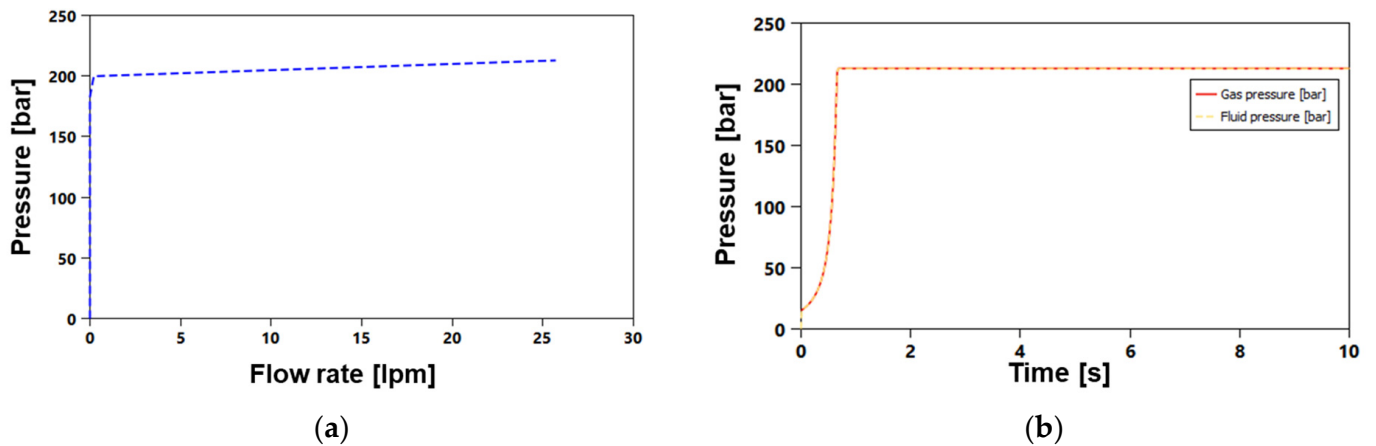


Figure 3. The hydraulic component design for the partial PST tractor. (a) Relief valve, (b) accumulator.

2.3.2. Engine Characteristic Map

The static torque of the engine is a function of the rotational speed and throttle opening of the engine [11]. The theoretical model of the engine static torque is in Equation (1).

$$T_e = f(n_e, \alpha), \tag{1}$$

where T_e is the torque of the engine (Nm); n_e is the rotational speed of the engine (rpm); and α is the throttle opening of the engine (%).

The throttle level of the engine controls the engine power by regulating the amount of fuel that enters the engine. The throttle opening of the engine is subjected to the throttle angles [25,30]. The engine map was designed for 100% load condition and Equation (1) was used to calculate the engine torque at each throttle level. The maximum torque for 100% throttle opening was found to be at around 500 Nm at an engine speed of 1600 rpm. The developed engine map was applied to conduct the simulation, which is shown in Figure 4.

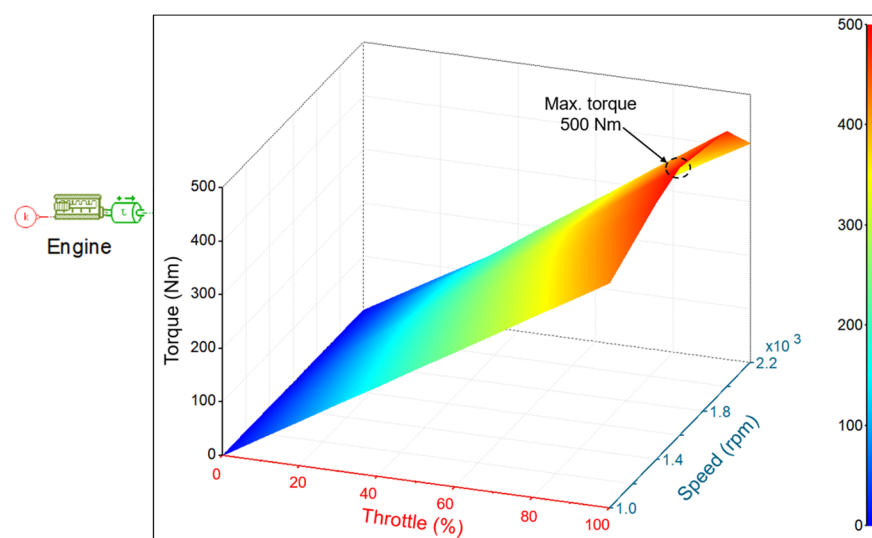


Figure 4. The 95-kW engine characteristics map used in this study.

2.3.3. Command Current of Proportional Valve

The proportional valve is used for engaging or disengaging the forward and reverse, Hi and Low, and three main clutches. Therefore, a total of 7 proportional valves (Figure 5a) were used in this simulation model. The power was supplied to the TCU (tractor control unit). The TCU supplied current to the proportional valve in response to the command current signal profile. In the case of a real tractor, the tuned command current profile that is already set up in the tractor, can modify using sensor setting curve connecting the notebook with CAN bus. The command current profile is shown in Figure 5b. The command current has three phases: (i) Fill phase (fill current to fill the clutch's internal empty volume); (ii) slip phase (slip current during slip between the friction and separate plates); and (iii) lockup phase (lockup current for the fully engaged clutch). The maximum command current was 1200 mA.

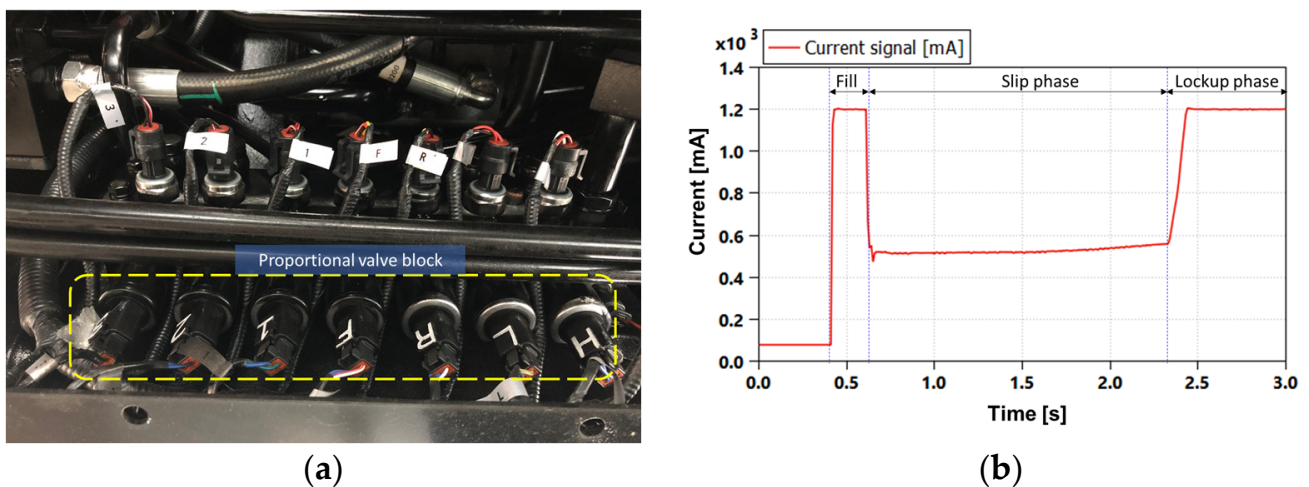


Figure 5. Proportional valves assembly with command current signal. (a) Proportional valve block of T130, (b) command signal of proportional valve.

2.3.4. Axle Load Condition

The measured axle loads for asphalt driving, plow, and rotary tillage were used as input load profile to verify the model developed and make a realistic estimation with an actual tractor. Also, the axle load can differentiate each field's operational condition in the simulation model. Figure 6 shows front left axle torque for asphalt driving, plow, and rotary tillage. During analysis, the fuel consumption during the operation period was considered. Therefore, the load profile was also considered only during the operation period.

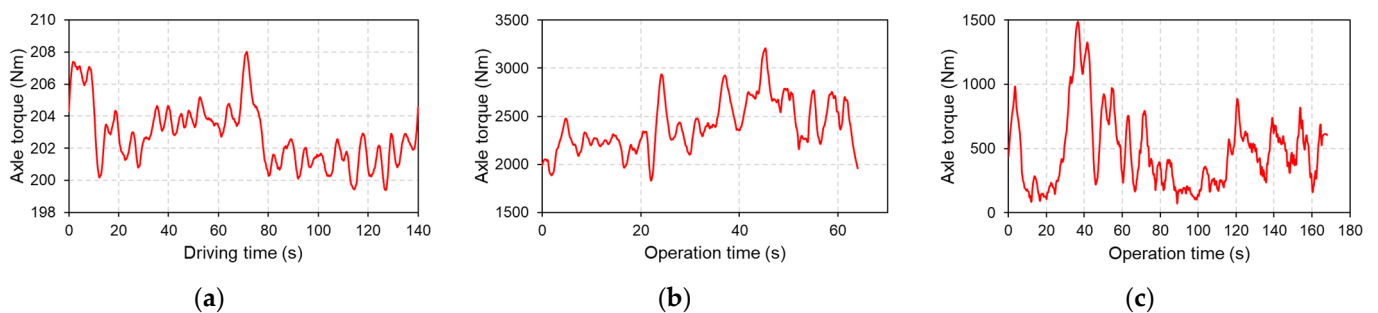


Figure 6. Axle loads of the target partial PST tractor during operations. (a) Asphalt driving, (b) plow tillage, (c) rotary tillage.

2.4. Experimental Conditions

2.4.1. Operational Condition

The field experiment was conducted for the engine mode of traditional, APS (Auto Power Shift) ECO, and APS power mode for asphalt driving, plow, and rotary tillage. Each operation was replicated 3 times to compare the fuel economic mode of operation. The field experiments for asphalt, plow, and rotary are shown in Figure 7. The operations were conducted at a maximum rotational speed of 2300 rpm in the engine traditional mode. In case of the APS ECO mode, the engine speed was set to 1400 rpm, whereas 1800 rpm of engine rotational speed was set for APS power mode. The field operation conditions are listed in Table 3.



Figure 7. The experiment using a 95-kW partial PST tractor.

Table 3. The experimental operation conditions of a partial PST tractor.

Operations	Engine Mode	Gear Stages (Speed)
Asphalt	Traditional	H3 (2300)
	APS ECO	H5 (1400)
	APS Power	H4 (1800)
Plow tillage	Traditional	M3 (2300)
	APS ECO	H5 (1400)
	APS Power	H4 (1800)
Rotary tillage	Traditional	L3 (2300)
	APS ECO	H5 (1400)
	APS Power	H4 (1800)

2.4.2. Experimental Site Condition

To test the field operation of the tractor, the experimental site Jeonju (RDA research field, Korea) was selected. Soil samples from the experimental site were collected and the soil texture was analyzed to determine the field condition using the USDA soil texture triangle, the hardness of the soil (Cone index, CI), and the electrical conductivity (EC). The soil samples were collected randomly at 5 points of each experimental site and physical and mechanical properties were measured. The soil analysis results for both fields are listed in Table 4.

Table 4. Soil analysis of the experimental site.

Parameter	Sand	Silt	Clay
Soil component (%)	62	22	16
Soil texture		Sandy loam	
Electric conductivity (dS/m)		0.46	
Cone index (kPa)		3306.8	

2.5. Statistical Analysis

Fuel consumption rates of the tractor for various engine modes were statistically analyzed for asphalt driving, plow, and rotary tillage. The error and accuracy of the fuel consumption rate for various engine modes were analyzed for both simulation and

experimental approaches by regression methods using IBM SPSS Statistics (SPSS 25, SPSS Inc., New York, NY, USA). The R-squared value was determined and values over 0.90 were considered reliable [31]. R-squared can be obtained using Equation (2).

$$R^2 = 1 - \frac{\sum_i (y_i - \hat{y}_i)^2}{\sum_i (y_i - \bar{y})^2}, \quad (2)$$

where R^2 is the regression coefficient of the fuel consumption rate for both methods; y_i is the i th measured fuel consumption rate (kg/h); \hat{y}_i is the i th simulation fuel consumption rate (kg/h), and \bar{y} is the mean of the measured fuel consumption (kg/h).

3. Results

3.1. Fuel Consumption Analysis

3.1.1. Asphalt Driving Operations

Fuel consumption tests for asphalt driving at gear stage H3 (traditional), H5 (APS ECO), and H4 (APS power) were conducted. It was observed that the fuel consumption rate was the highest with the traditional engine mode at maximum rotational speed of 2300 rpm, accounting for averages of 10.86 and 11.12 kg/h for measured and simulation, respectively. The lowest fuel consumption rate was found at H5 (APS ECO engine mode) for 1350 rpm speed, where the measured and simulation average fuel consumptions were almost 6.00 and 6.67 kg/h, respectively. The fuel consumption rates at various engine modes were listed in Table 5.

Table 5. Fuel consumption analysis during asphalt driving.

Gear Stages (Mode)	Setting Speed (rpm)	Replications	Fuel Consumption	
			Measured (kg/h)	Simulation (kg/h)
H3 (Traditional)	2300	1	11.03	11.25
		2	10.85	11.17
		3	10.72	10.93
		Average	10.86	11.12
H5 (APS ECO)	1350	1	6.00	7.86
		2	6.00	6.18
		3	6.02	5.96
		Average	6.00	6.67
H4 (APS Power)	1750	1	7.62	7.74
		2	7.67	7.60
		3	7.63	7.74
		Average	7.64	7.69
Traditional vs APS ECO (%)			44.73	40.05
Traditional vs APS power (%)			21.42	13.35

In the comparison among engine modes, it was observed that the fuel consumption with the APS ECO mode for both measured and simulation were the most economic compared to traditional mode, accounting for around 44.73 and 40.05%, respectively. It was also observed that fuel consumption with APS power mode for both measured and simulation were almost 21.42 and 13.35%, respectively, which is more economic than the traditional mode. The statistical analysis shows that the simulation and measured fuel consumptions were linearly correlated, with an R^2 of 0.9845. The statistical analysis results are shown in Figure 8.

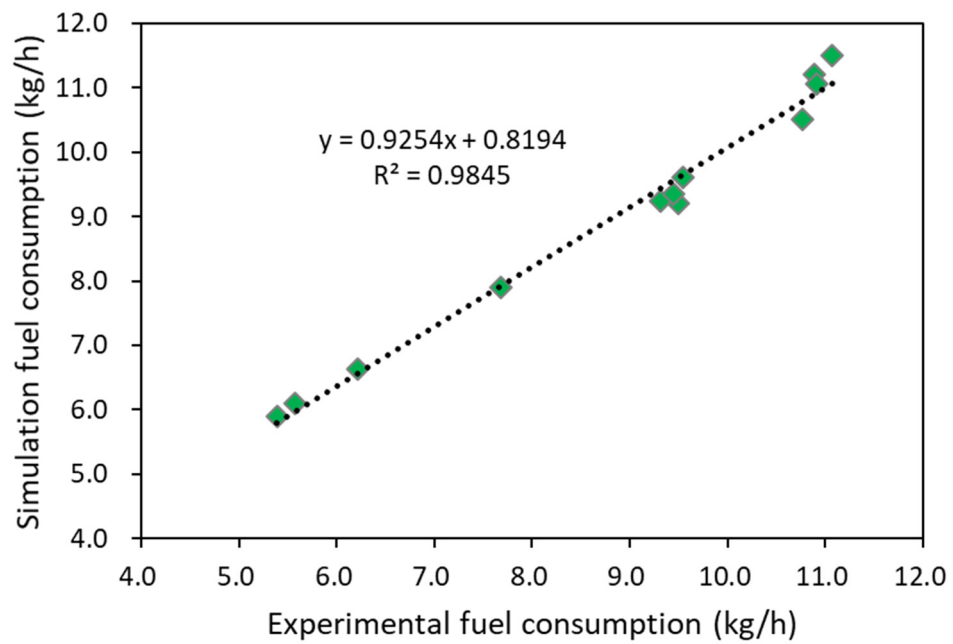


Figure 8. Regression analysis of fuel consumption during asphalt operation.

3.1.2. Plow Tillage

Fuel consumption tests for plow tillage at gear stage M3 (traditional), M4 (APS ECO), and M4 (APS power) were conducted. The highest average fuel consumptions for the traditional mode were approximately 20.2 and 20.0 kg/h for measured and simulation, respectively. The lowest measured and simulation average fuel consumptions at M4 (APS ECO engine mode) for 1650 rpm speed were almost 14.9 and 15 kg/h, respectively. The fuel consumption rates at various engine modes were listed in Table 6.

Table 6. Fuel consumption analysis during plow tillage.

Gear Stage (Mode)	Setting Speed (rpm)	Replications	Fuel Consumption	
			Measured (kg/h)	Simulation (kg/h)
M3 (Traditional)	2300	1	19.8	19.3
		2	21.4	21.2
		3	19.3	19.5
		Average	20.2	20.0
M4 (APS ECO)	1650	1	15.4	15.5
		2	15.5	15.8
		3	13.9	13.7
		Average	14.9	15.0
M4 (APS Power)	1800	1	18.0	18.1
		2	17.6	17.4
		3	17.5	17.6
		4	16.4	16.3
		Average	17.4	17.4
Traditional vs APS ECO (%)			25.89	25.17
Traditional vs APS power (%)			19.64	13.25

In the comparison among engine modes, it was observed that the fuel consumption with the APS ECO mode for measured and simulation were the most economic compared to the traditional mode, accounting for around 25.89 and 25.17%, respectively. It was also

observed that fuel consumption with APS power mode for both measured and simulation were almost 19.64 and 13.25%, respectively, which was more economic than the traditional mode. The statistical analysis shows that the simulation and measured fuel consumptions were linearly correlated, with an R^2 of 0.992. The statistical analysis results are shown in Figure 9.

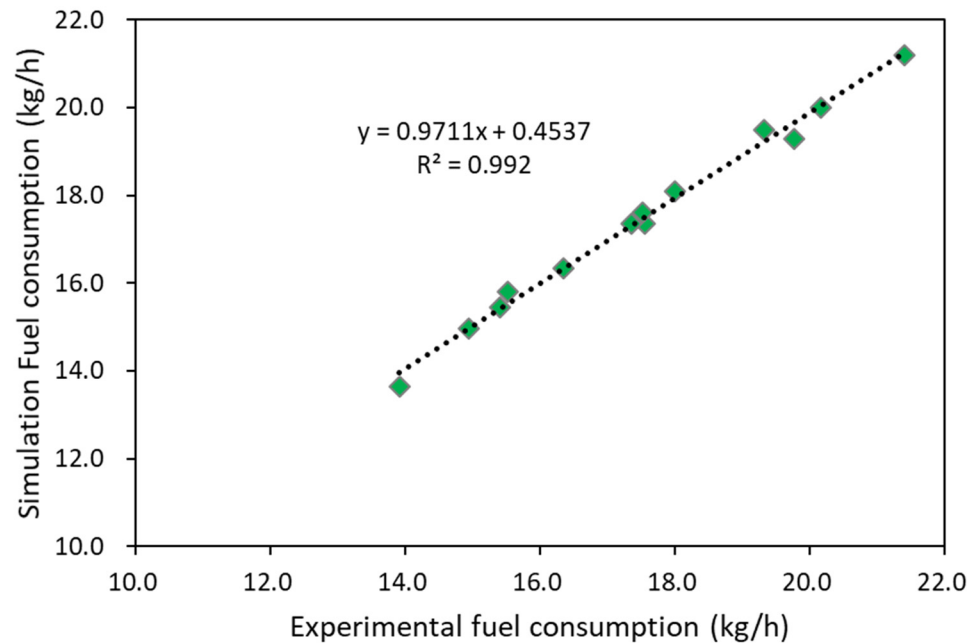


Figure 9. Regression analysis of fuel consumption during plow tillage.

3.1.3. Rotary Tillage

Fuel consumption tests for rotary tillage at gear stage L3 (traditional), L4 (APS ECO), and L4 (APS power) were conducted. The highest fuel consumption was with the traditional mode of engine, accounting for averages of 23.1 and 22.8 kg/h for measured and simulation, respectively. The lowest fuel consumption rates were found to be almost 13.3 and 13.2 kg/h at L4 (APS ECO engine mode) for measured and simulation, respectively. The fuel consumption rates at various engine modes were listed in Table 7.

Table 7. Fuel consumption analysis during rotary tillage.

Gear Stage (Mode)	Setting Speed (rpm)	Replications	Fuel Consumption	
			Measured (kg/h)	Simulation (kg/h)
L3 (Traditional)	2300	1	22.8	22.2
		2	23.9	23.7
		3	22.5	22.6
		Average	23.1	22.8
L4 (APS ECO)	1650	1	13.2	13.1
		2	12.9	12.7
		3	13.8	13.9
		Average	13.3	13.2

Table 7. Cont.

Gear Stage (Mode)	Setting Speed (rpm)	Replications	Fuel Consumption	
			Measured (kg/h)	Simulation (kg/h)
L4 (APS Power)	1800	1	17.5	17.4
		2	15.2	15.9
		3	16.8	16.7
Average			16.5	16.6
Traditional vs APS ECO (%)			42.35	42.06
Traditional vs APS power (%)			28.41	27.04

In the comparison among engine modes, it was observed that fuel consumption with the APS ECO mode for both measured and simulation were more economic compared to the traditional mode, accounting for around 42.35 and 42.06%, respectively. It was also observed that fuel consumption with the APS power mode for both measured and simulation were almost 28.41 and 27.04%, respectively, which was more economic than the traditional mode. The statistical analysis shows that the simulation and measured fuel consumptions were linearly correlated, with an R^2 of 0.9955. The statistical analysis results are shown in Figure 10.

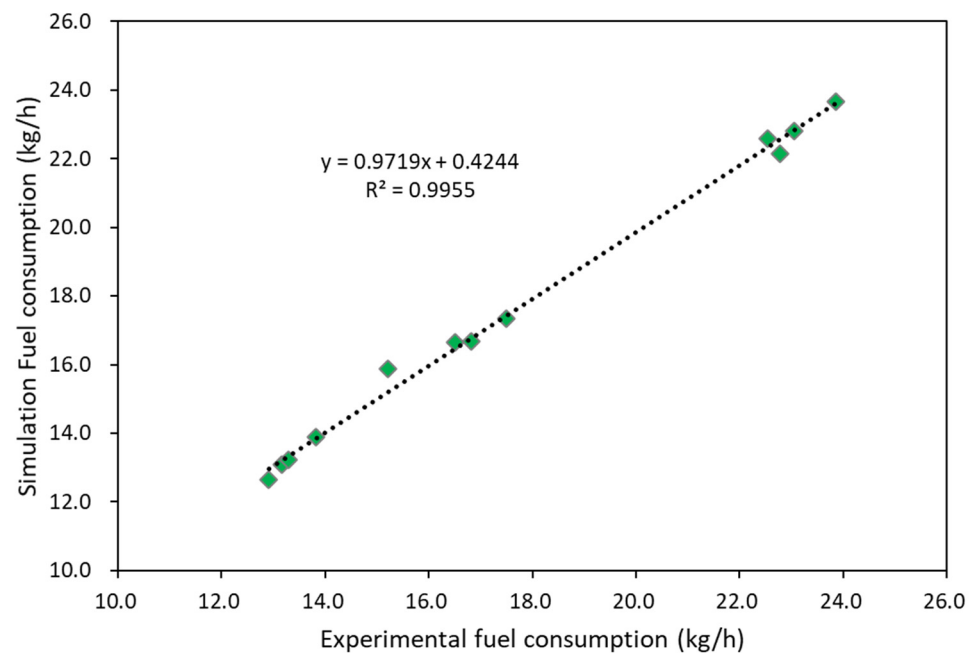


Figure 10. Regression analysis of fuel consumption during rotary tillage.

3.2. Performance Evaluation

To generalize our model for actual operations, it is necessary to consider low fuel consumption rate and high torque. Therefore, the experimental load generated during asphalt driving, plow, and rotary tillage at various engine modes were plotted in the performance curve, which is shown Figure 11. Fuel consumption was gradually increased after an engine speed of 1500 rpm. This indicates that the engine should run at a low speed to minimize fuel consumption. However, tractor working efficiency would be decreased at a low speed. It may unexpectedly be turned off the engine due to the load variation. For this reason, the engine speed should remain under the ungoverned region. The efficiency was comparatively high but the fuel consumption was relatively lower.

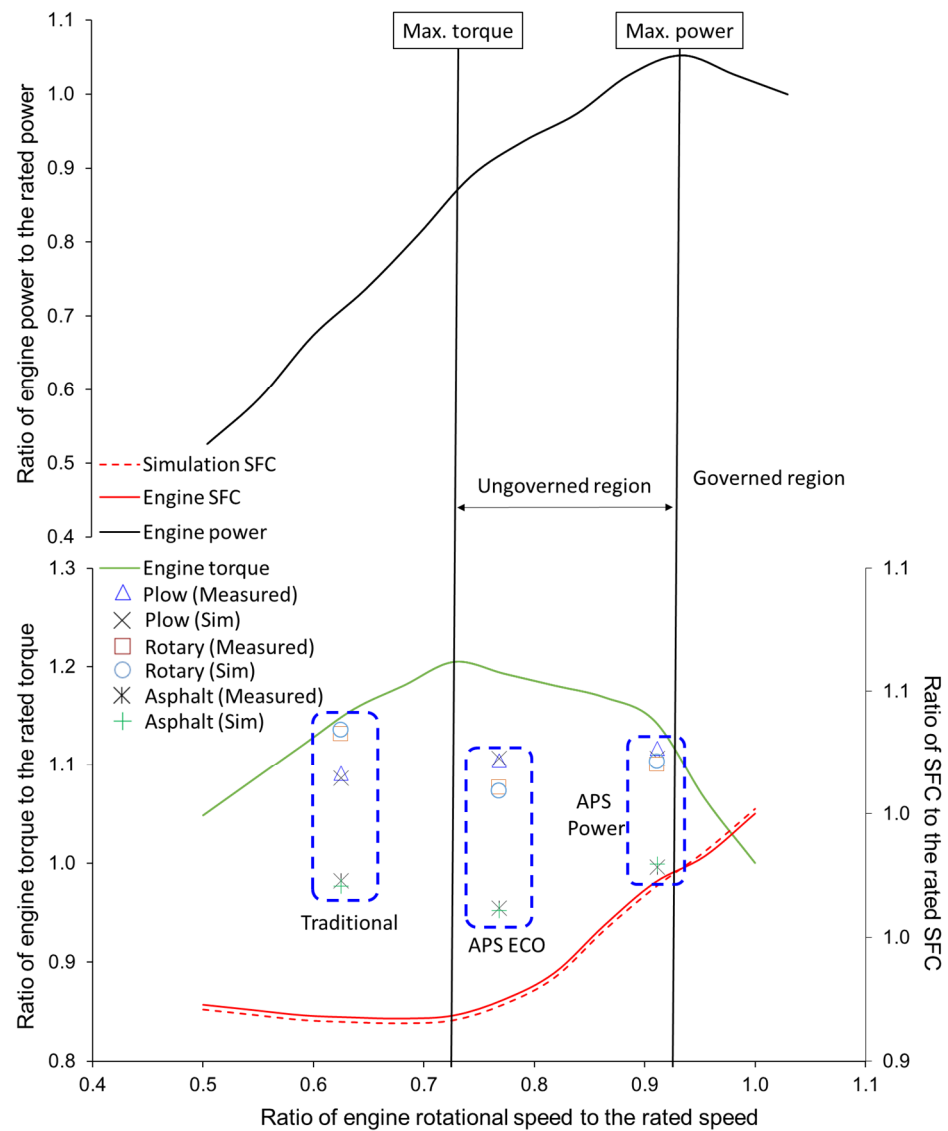


Figure 11. Performance evaluation of a partial PST tractor during asphalt, plow, and rotary tillage.

It is clearly observed that the engine loads remain in the ungoverned zone for the APS ECO and APS power modes at all gear stages for asphalt driving, plow, and rotary tillage. However, APS power mode consumes higher fuel compared to APS ECO. Therefore, it is suggested to the users to operate the tractor in the APS ECO mode for high fuel economy and reasonable working loads.

4. Conclusions

This study focused on the verification and performance evaluation of the simulation model of a partial PST tractor for various engine modes during field operations. A 95-kW partial PST tractor was used to evaluate the simulation model and perform the field experiment. The simulation model was verified using the asphalt driving condition and evaluated the performance for plow and rotary tillage at different engine modes. Finally, the most suitable and economic gear stages or engine modes were suggested to users for field operations. The overall findings of the study are listed below:

1. Fuel consumption in the APS ECO engine mode for both measured and simulation were highly economic in comparison with the traditional engine mode, which were accounting for approximately 44.73 and 40.05%, respectively. Between the APS ECO and APS power modes, APS ECO was also more economic compared to APS power,

accounting for around 21.42 and 13.35% for measured and simulation, respectively. The statistical analysis showed that both experimental and simulation results were linearly correlated, with an R^2 of 0.9845.

2. In the plow tillage case, it was found that fuel consumption for the APS ECO engine mode was the most economic compared to traditional and APS power engine modes. The fuel consumption in the APS ECO mode for measured and simulation were around 25.89 and 25.17%, respectively compared to the traditional mode; in APS power mode, measured and simulation were almost 19.64 and 13.25%, respectively compared to the traditional mode. The statistical analysis shows that the simulation and measured fuel consumptions were in linear relation, with an R^2 of 0.992.
3. In the comparison among engine modes during rotary tillage, it was observed that the fuel consumption in the APS ECO mode for both measured and simulation were the most economic compared to the traditional mode, accounting for around 42.35 and 42.06%, respectively. It was also observed that fuel consumption in the APS power mode for measured and simulation were almost 28.41 and 27.04%, respectively, which was also economic than the traditional mode. The statistical analysis shows that the simulation and measured fuel consumptions were in linear relation, with an R^2 of 0.9955.
4. It is clearly observed that the engine loads remain in the ungoverned zone for the APS ECO and APS power modes at all gear stages for asphalt driving, plow, and rotary tillage. However, the APS power mode consumes more fuel compared to APS ECO. Therefore, it is suggested to users to operate the tractor in APS ECO mode for high fuel economy and reasonable working loads.

In summary, according to the statistical analysis, the simulation model was verified in the asphalt driving condition and the model was performed with accuracy as the experimental and simulation results were in a linear relationship with accuracy of over 98%. It was observed that the APS ECO engine mode is highly fuel economic compared to the traditional and APS power modes. Therefore, it could be suggested that users should perform the operations using the partial PST tractor in the APS ECO engine mode to improve fuel consumption.

Author Contributions: Conceptualization, M.A.A.S., R.-G.L. and Y.-J.K.; methodology, M.A.A.S., S.-M.B. and S.-Y.B.; software, M.A.A.S.; validation, M.A.A.S., S.-Y.B. and S.-M.B.; formal analysis, M.A.A.S.; investigation, R.-G.L. and Y.-J.K.; writing—original draft preparation, M.A.A.S.; writing—review and editing, M.A.A.S.; visualization, M.A.A.S., R.-G.L. and Y.-J.K.; supervision, Y.-J.K. and R.-G.L.; project administration, Y.-J.K.; funding acquisition, Y.-J.K. All authors have read and agreed to the published version of the manuscript.

Funding: This work was supported by the Korea Institute of Planning and Evaluation for Technology in Food, Agriculture and Forestry (IPET) through the Advanced Production Technology Development Program, funded by the Ministry of Agriculture, Food and Rural Affairs (MAFRA) (320080-3). It was also supported by the Korea Institute of Planning and Evaluation for Technology in Food, Agriculture and Forestry (IPET) thorough Technology Commercialization Support Program, funded by Ministry of Agriculture, Food and Rural Affairs (MAFRA) (821014-03).

Institutional Review Board Statement: Not applicable.

Informed Consent Statement: Not applicable.

Data Availability Statement: Data are presented in this article in the form of figures and tables.

Conflicts of Interest: The authors declare no conflict of interest.

References

1. Tanelli, M.; Panzani, G.; Savaresi, S.M.; Pirola, C. Transmission Control for Power-Shift Agricultural Tractors: Design and End-of-Line Automatic Tuning. *Mechatronics* **2011**, *21*, 285–297. [[CrossRef](#)]
2. Baek, S.M.; Kim, W.S.; Kim, Y.S.; Baek, S.Y.; Kim, Y.J. Development of a Simulation Model for HMT of a 50 kW Class Agricultural Tractor. *Appl. Sci.* **2020**, *10*, 4064. [[CrossRef](#)]

3. Kim, W.S.; Kim, Y.J.; Kim, Y.S.; Baek, S.Y.; Baek, S.M.; Lee, D.H.; Nam, K.C.; Kim, T.B.; Lee, H.J. Development of Control System for Automated Manual Transmission of 45-kW Agricultural Tractor. *Appl. Sci.* **2020**, *10*, 2930. [[CrossRef](#)]
4. Liyou, X.; Yihao, Z.; Jinzhong, S.; Xianghai, Y. Optimization of Power Shift Tractor Clutch Based on Ahp and Improved Genetic Algorithm. *Acta Tech.* **2017**, *62*, 373–384.
5. Liang, J.; Yang, H.; Wu, J.; Zhang, N.; Walker, P.D. Power-on Shifting in Dual Input Clutchless Power-Shifting Transmission for Electric Vehicles. *Mech. Mach. Theory* **2018**, *121*, 487–501. [[CrossRef](#)]
6. Siddique, M.A.A.; Kim, T.J.; Kim, Y.J. Technical Trend of the Power Shift Transmission (PST) of Agricultural Tractor. *J. Drive Control* **2020**, *17*, 68–75.
7. Neto, L.S.; Zimmermann, G.G.; Jasper, S.P.; Savi, D.; Sobenko, L.R. Energy Efficiency of Agricultural Tractors Equipped with Continuously Variable and Full Powershift Transmission Systems. *Eng. Agric.* **2022**, *42*, e20210052. [[CrossRef](#)]
8. Li, C.; Ke, M.; Wu, Y. Research and Implementation of Tractor Power Shift Clutch Control System. *MATEC Web Conf.* **2018**, *153*, 04003. [[CrossRef](#)]
9. Ngo, D.V.; Hofman, T.; Steinbuch, M.; Serrarens, A.; Merckx, L. Improvement of Fuel Economy in Power-Shift Automated Manual Transmission through Shift Strategy Optimization—An Experimental Study. In Proceedings of the 2010 IEEE Vehicle Power and Propulsion Conference, Lille, France, 1–3 September 2010; IEEE: Piscataway, NJ, USA, 2010; pp. 1–5. [[CrossRef](#)]
10. Molari, G.; Sedoni, E. Experimental Evaluation of Power Losses in a Power-Shift Agricultural Tractor Transmission. *Biosyst. Eng.* **2008**, *100*, 177–183. [[CrossRef](#)]
11. Li, B.; Sun, D.; Hu, M.; Liu, J. Research on Economic Comprehensive Control Strategies of Tractor-Planter Combinations in Planting, Including Gear-Shift and Cruise Control. *Energies* **2018**, *11*, 686. [[CrossRef](#)]
12. Li, B.; Sun, D.; Hu, M.; Liu, J. Automatic Starting Control of Tractor with a Novel Power-Shift Transmission. *Mech. Mach. Theory* **2019**, *131*, 75–91. [[CrossRef](#)]
13. Holgerson, M. Influence of Operating Conditions on Friction and Temperature Characteristics of a Wet Clutch Engagement. *Tribol. Test* **2000**, *7*, 99–114. [[CrossRef](#)]
14. Siddique, M.A.A.; Kim, W.S.; Kim, Y.S.; Kim, T.J.; Choi, C.H.; Lee, H.J.; Chung, S.O.; Kim, Y.J. Effects of Temperatures and Viscosity of the Hydraulic Oils on the Proportional Valve for a Rice Transplanter Based on PID Control Algorithm. *Agriculture* **2020**, *10*, 73. [[CrossRef](#)]
15. Siddique, M.A.A.; Kim, W.S.; Baek, S.Y.; Kim, Y.J.; Park, S.U.; Choi, C.H.; Choi, Y.S. Analysis of the Axle Load of a Rice Transplanter According to Gear Selection. *J. Drive Control* **2020**, *17*, 125–132. [[CrossRef](#)]
16. Raikwar, S.; Tewari, V.K.; Mukhopadhyay, S.; Verma, C.R.B.; Sreenivasulu Rao, M. Simulation of Components of a Power Shuttle Transmission System for an Agricultural Tractor. *Comput. Electron. Agric.* **2015**, *114*, 114–124. [[CrossRef](#)]
17. Li, B.; Sun, D.; Hu, M.; Zhou, X.; Liu, J.; Wang, D. Coordinated Control of Gear Shifting Process with Multiple Clutches for Power-Shift Transmission. *Mech. Mach. Theory* **2019**, *140*, 274–291. [[CrossRef](#)]
18. Yiwei, W.; Xianghai, Y.; Zhili, Z. Architecture Modeling and Test of Tractor Power Shift Transmission. *IEEE Access* **2021**, *9*, 3517–3525. [[CrossRef](#)]
19. Yang, S.; Bao, Y.; Fan, C. Study on Characteristics of Hydro-Mechanical Transmission in Full Power Shift. *Adv. Mech. Eng.* **2018**, *10*, 1687814018790668. [[CrossRef](#)]
20. Wang, F.; Wang, Y.; Han, J.H.; Yao, J. Experimental and Simulated Studies on Hydraulic Buffering Valve for ZF-4WG308 Power-Shift Transmission. *J. Cent. South Univ.* **2017**, *24*, 1801–1807. [[CrossRef](#)]
21. Wu, Y.; Mao, Y.; Xu, L. FMI-Based Co-Simulation Method and Test Verification for Tractor Power-Shift Transmission. *PLoS ONE* **2022**, *17*, e0263838. [[CrossRef](#)]
22. Song, L.; Xu, L.; Liu, M. Research on the Law of Dynamic Shifting and Coordinated Section Shifting of Tractor Full-Power Shift Transmission. *J. Phys. Conf. Ser.* **2022**, *2343*, 012021. [[CrossRef](#)]
23. Xia, G.; Chen, J.; Tang, X.; Zhao, L.; Sun, B. Shift Quality Optimization Control of Power Shift Transmission Based on Particle Swarm Optimization—Genetic Algorithm. *J. Automob. Eng.* **2021**, *236*, 872–892. [[CrossRef](#)]
24. Wang, H.; Ma, B.; Niu, L.; Zheng, C. The Wear Characteristics of Thrust Washer in Conflux Planetary Gear Train of Power Shift Transmission. *Eng. Fail. Anal.* **2013**, *28*, 318–327. [[CrossRef](#)]
25. Siddique, M.A.A.; Kim, W.S.; Kim, Y.S.; Baek, S.Y.; Baek, S.M.; Kim, Y.J.; Park, S.U.; Choi, C.H. Simulation of Design Factors of a Clutch Pack for Power-Shift Transmission for an Agricultural Tractor. *Sensors* **2020**, *20*, 7293. [[CrossRef](#)]
26. Yamaguchi, T.; Ando, J.; Tsuda, T.; Takahashi, N.; Tohyama, M.; Murase, A.; Ohmori, T.; Hokkirigawa, K. Sliding Velocity Dependency of the Friction Coefficient of Si-Containing Diamond-like Carbon Film under Oil Lubricated Condition. *Tribol. Int.* **2011**, *44*, 1296–1303. [[CrossRef](#)]
27. Fatima, N.; Marklund, P.; Larsson, R. Influence of Clutch Output Shaft Inertia and Stiffness on the Performance of the Wet Clutch. *Tribol. Trans.* **2013**, *56*, 310–319. [[CrossRef](#)]
28. Abdullah, O.I.; Schlattmann, J. The Effect of Disc Radius on Heat Flux and Temperature Distribution in Friction Clutches. *Adv. Mat. Res.* **2012**, *505*, 154–164. [[CrossRef](#)]
29. Siddique, M.A.A.; Baek, S.M.; Baek, S.Y.; Kim, W.S.; Kim, Y.S.; Kim, Y.J.; Lee, D.H.; Lee, K.H.; Hwang, J.Y. Simulation of Fuel Consumption Based on Engine Load Level of a 95 kW Partial Power-Shift Transmission Tractor. *Agriculture* **2021**, *11*, 276. [[CrossRef](#)]

30. Bera, P. Torque Characteristic of SI Engine in Dynamic Operating States. *Combust. Engines* **2017**, *171*, 175–180. [[CrossRef](#)]
31. Shafaei, S.M.; Kamgar, S. A Comprehensive Investigation on Static and Dynamic Friction Coefficients of Wheat Grain with the Adoption of Statistical Analysis. *J. Adv. Res.* **2017**, *8*, 351–361. [[CrossRef](#)]

Disclaimer/Publisher's Note: The statements, opinions and data contained in all publications are solely those of the individual author(s) and contributor(s) and not of MDPI and/or the editor(s). MDPI and/or the editor(s) disclaim responsibility for any injury to people or property resulting from any ideas, methods, instructions or products referred to in the content.